HOKKAIDO UNIVERSITY

Title	Spherical turbulent flame propagation of pulverized coal particle clouds in an O_2/N_2 atmosphere
Author(s)	Hadi, Khalid; Ichimura, Ryo; Hashimoto, Nozomu; Fujita, Osamu
Citation	Proceedings of the Combustion Institute, 37(3), 2935-2942 https://doi.org/10.1016/j.proci.2018.09.021
Issue Date	2019-01
Doc URL	http://hdl.handle.net/2115/81987
Rights	© 2018. This manuscript version is made available under the CC-BY-NC-ND 4.0 license http://creativecommons.org/licenses/by-nc-nd/4.0/
Rights(URL)	http://creativecommons.org/licenses/by-nc-nd/4.0/
Type	article (author version)
File Information	PCI_PROCI-D-17-01587R3.pdf

Instructions for use

Hokkaido University Collection of Scholarly and Academic Papers : HUSCAP

[Title Page]

1. **Spherical turbulent flame propagation of pulverized coal particle clouds in an O_2/N_2 atmosphere**

2. Author (s) : Khalid Hadi, Ryo Ichimura, Nozomu Hashimoto, Osamu Fujita

Division of Mechanical and Space Engineering, Hokkaido University,

Kita13 Nishi8, Kita-ku, Sapporo 060-8628, Japan

3. Corresponding author information:

Nozomu Hashimoto*

Professor, Hokkaido University,

Kita13 Nishi8, Kita-ku, Sapporo 060-8628, Japan

E-mail address: nozomu.hashimoto@eng.hokudai.ac.jp

Tel.: +81-11-706-6386; Fax: +81-11-706-7841

4. Colloquium : Solid fuel combustion

5. Total length of paper : 6196 (word count via method 1)

6. List word equivalent lengths

Body: 3272

Equations: 46

Reference: 385

Table: 144

Figures: 2349 [167 + 129 + 131 + 140 + 181 + 283 + 130+ 138 + 525+525 (for Fig. 1-10 with captions)]

7. Affirmation to pay color reproduction charges (if applicable) : No

Abstract

This study aimed to clarify the effects of turbulence intensity and coal concentration on the spherical turbulent flame propagation of a pulverized coal particle cloud. A unique experimental apparatus was developed in which coal particles can be dispersed homogeneously in a turbulent flow field generated by two fans. Experiments of spherical turbulent flame propagation of pulverized coal particle clouds in a constant volume spherical chamber in various turbulence intensities and coal concentrations were conducted using the new experimental apparatus. A common bituminous coal was used in this study. Flame propagation velocity was obtained based on the analysis of flame propagation images taken using a high-speed camera. It was found that the flame propagation velocity increased with increasing flame radius. For various turbulence intensities, the flame propagation velocity increases as the turbulence intensity increases. Similar trends were observed in spherical flames using gaseous fuel. The coal concentration has a weak effect on the flame propagation velocity, which is a feature that is unique to pulverized coal flames in a turbulent field. Experimental results of a spherical flame propagation behavior of turbulent pulverized coal particle cloud have been reported for the first time. The results obtained in this study are obviously different from previous pulverized coal combustion studies and any other results of gaseous fuel combustion research.

---

* Corresponding author: Tel.: +81-11-706-6386. E-mail address: nozomu.hashimoto@eng.hokudai.ac.jp

Keywords: Coal combustion; Flame propagation; Turbulence intensity; Spherical flame; Turbulent combustion

List of figure captions

Figure 1	Schematic of experimental apparatus.
Figure 2	Equipment of PIV measurement.
Figure 3	Turbulence intensity, u' as a function of fan speed, N.
Figure 4	Variation of longitudinal velocity correlation coefficient, $R_{11}(x)$, with distance, x.
Figure 5	Flame propagation in 40% O_2 and 60% N_2 mixture for G = 2.0 kg/m^3.
Figure 6	Spark images (a) without coal particle cloud (in air) and (b) with coal particle cloud (u' = 0.32 m/s, G = 2.0 kg/m^3).
Figure 7	Pressure history during flame propagation.
Figure 8	Flame radius time histories for G = 2.0 kg/m³ in various turbulence intensity, u'.
Figure 9	Relationship between flame propagation velocity and flame radius for a) u'= 0.32 m/s, b) u'= 0.65 m/s , c) u'= 0.97 m/s and d) u'=1.29 m/s.
Figure 10	Flame propagation velocity at various turbulence intensities, u' for a) G of 0.3 and 0.6 kg/m³, b) G =1.3 kg/m³, c) G = 2.0 kg/m³ and d) G = 2.3 kg/m³.

1. Introduction

Among the various fossil fuels, coal continues to serve as an important energy source because there remains an abundant supply of accessible deposits worldwide. Pulverized coal, which is utilized in many thermal-power stations, is a particularly important example of the application of coal-power production; therefore, a fundamental understanding of the combustion characteristics of pulverized coal is necessary to improve fuel usage efficiency. In many thermal-power plants, coal-fired boilers combust pulverized coal particles in a turbulent environment. In such plants, the flame propagation behavior is one of the most important properties for the flame stability of the burner [1]. The pyrolysis rate and the amount of volatile matter generated strongly affect the flame stability [2].

It is well known that the mechanism of pulverized coal combustion are more complex compared to that of gaseous or liquid fuels because the particle devolatilization and chemical reaction processes occur simultaneously. A number of experimental and numerical studies on pulverized coal combustion have already been conducted. Fujita et al. [3], Kiga et al. [4], and Suda et al. [1] investigated the characteristics of quiescent pulverized coal cloud combustion in a microgravity environment. Other studies investigated turbulent pulverized coal combustion in jet flames [5,6]. Hayashi et al. [7] and Hashimoto et al. [8] explored soot formation characteristics in a lab-scale turbulent pulverized coal flame. Taniguchi et al. [9] studied flame propagation behavior of a pulverized coal cloud in a laminar upward flow. Kruger et al. [10] investigated the effect of turbulence on char particle reactivity. However, the effects of turbulence intensity and coal particle concentration on the flame propagation behavior of pulverized coal particles have not yet been reported. It is expected that the pulverized coal combustion mechanism in a turbulent environment may differ from that in quiescent or laminar flow. Moreover, the authors are not aware of any previous papers that report on the effect of coal particle concentration on flame propagation behavior in a turbulent environment.

Spherically propagating premixed flames have been investigated to clarify the fundamental characteristics of premixed flames for gaseous fuels in a constant volume combustion chamber. Smallbone et al. [11], Kitagawa et al. [12] and Hayakawa et al. [13] reported the burning velocities of

spherically propagating flames under laminar and turbulent flow for various conditions. Tse et al. [14] investigated the propagation phenomena of spherically premixed flames under various conditions and pressures up to 60 atm. The more recent work of Goulier et al. [15] on laminar and turbulent flame velocity of premixed hydrogen/air mixtures suggested that a homogeneous and isotropic turbulence can be generated using several fans.

This study aims to clarify the effects of turbulence intensity and coal concentration on the spherical turbulent flame propagation of a pulverized coal particle cloud. Experiments were conducted under various coal particle concentrations at atmospheric pressure in a turbulent flow field generated by fans in a closed spherical vessel. New models for the flame propagation of a coal particle cloud may be developed based on the experimental results from this study.

2. Experimental apparatus and procedures

Experiments were performed using a constant volume spherical combustion chamber as shown in Fig.1. The inner diameter of the chamber is 200 mm and height is 280 mm. The total volume of the chamber is approximately 6.19×10^{-3} m^3. Although previous experimental studies for coal ignition utilized either a hot wire ignitor or a laser ignitor [1-4,9], this study employed a spark ignitor composed of two stainless steel electrodes with a diameter of 1.8 mm. A hot wire ignitor adds the undesirable effect of radiation on flame propagation, while a laser ignitor cannot penetrate the coal cloud to reach the center point of chamber used in this study. Furthermore, the ignition energy cannot be easily measured due to laser light scattering by coal particles. One of the advantages of using a spark ignitor is that there is almost no effect of spark on the flame propagation behavior after the ignition affected period. Another advantage is that the spark electrode is easily installed at the desired position and more accurate ignition timing is gurauranteed. The spark gap was set to 2 mm. In general, a spark gap between 1-3 mm is suitable for generating accurate spark ignition energy [16]. A capacitor discharge ignition (CDI) circuit was adopted for spark ignition. A series of capacitors with a total of 50 μF were charged by a 469 VDC in the CDI circuit. A total spark energy of 5.5 J was discharged to the ignition

coil to induce a spark at the center of chamber among the coal cloud, ensuring the ignition of pulverized coal particles. A turbulent flow field was generated in the chamber by the counter-rotation of two identical seven-bladed fans located vertically and symmetrically. The fans were coupled to 150 W motors equipped with encoders connected to ESCON50/5 controllers to control the rotational speeds of the fans.

The flame propagation of the pulverized coal particle clouds was observed by direct photography at sample rate of 1800 fps using a high-speed camera (Miro C with UV lens) through a 50-mm diameter quartz glass window. Pressure histories inside the chamber were measured using a Valcom VPRTF-A4 pressure sensor and recorded via a Hioki 8870 data logger. Another similar pressure sensor with a digital panel meter was employed for monitoring the gas mixture pressure in the dispersion tank.

Common bituminous pulverized coal particles with an average diameter of 48 μm on mass basis were used as fuel. The coal properties are shown in Table 1. Diluted oxygen (40 vol% O_2 and 60 vol% N_2) was used as the ambient gas to achieve flame propagation. Coal concentrations (G) inside the combustion chamber were set to 0.3, 0.6, 1.3, 2.0 and 2.3 kg/m³. According to work by Suda et al. [1], the highest flame propagation velocity of a quiescent pulverized coal particle cloud in a microgravity environment was obtained when the coal concentration was around 1.3 kg/m³. In this study, however, experiments were performed in a normal gravity environment, and flame propagation could only be observed at the coal concentration of 1.3 kg/m³.

Before fiiling the ambient gas, the combustion chamber and the dispersion tank were emptied via a vacuum pump. After emptying the tank, dispersion gas of 40 vol% O_2 and 60 vol% N_2 was stored in a dispersion tank at a total pressure of 300 kPa. The ambient gas was supplied to the combustion chamber to only 0.084 MPa to allow the pressure to reach 0.1 MPa after supplying the dispersion gas with coal particles. Coal particles were loaded into four filter cups and tubes corresponding to the symmetrical configuration of four inlets before initiating the dispersion. Coal particles were dispersed into the chamber simultaneously by the sweeping flow from the dispersion tank for 0.7 seconds. Just 0.3 seconds after the end of the dispersion, the mixture was ignited at 0.1 MPa. The fan rotation was started

approximately 3 minutes prior to dispersion and kept running at a constant (pre-specified) speed during the flame propagation. The mass of coal particles remaining in the filter cups and tubes after dispersion was measured to confirm the total mass of coal particles dispersed into the chamber. After each experiment, the chamber was opened by detaching the lid, and the inner chamber was cleaned. The maximum error for O_2 concentration, the total pressure inside the chamber, and the coal concentration are 1.2%, 5%, and 4%, respectively. According to the results of this study, the errors can be neglected in the final conclusion. The present technique was validated by performing quiescent ammonia/air premixed combustion at 0.1 MPa. For an equivalence ratio of 1.0, the laminar burning velocity from the present study is 6.85 cm/s, which is almost the same as that reported by Hayakawa et al.: 6.91 cm/s [17]. The minimum of three experimental data sets for each condition were used for analysis.

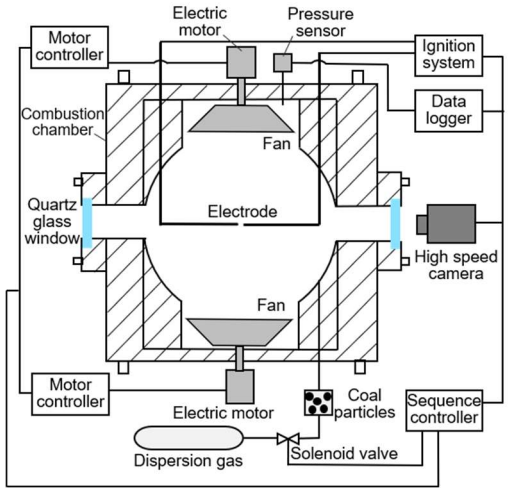

Fig. 1. Schematic of experimental apparatus.

Table 1
Physical and chemical analysis of coal

Analysis	Common bituminous coal
Proximate [wt%]	
Moisture[b]	0.7
Ash[a]	14.2
Volatile matter[a]	33.5
Fixed carbon[a]	52.3
Ultimate [wt%, dry]	
Carbon	70.5
Hydrogen	4.64
Nitrogen	1.66
Oxygen	8.59
Sulfur	0.46
Heating value [MJ/kg]	27.8

[a] Dry basis.
[b] As received.

2.1 Turbulence intensity and fan speed correlation

A correlation between fan rotational speed, N and turbulence intensity, u' was obtained from Particle Image Velocimetry (PIV) measurements carried out by Seika Digital Image Co., Ltd. The PIV measurement system consists of a CCD camera with 1600 × 1200 pixels resolution, a double-pulsed Nd:YAG laser of 532 nm wavelength with delay of 10 μs, a timing controller, and a seeding generator. Figure 2 shows the PIV measurement equipment. Oil mist with 1 μm sized particles was used as particle tracing seed. Various scales of turbulent eddies exist in a turbulent field, therefore MicroNikkor105mm f/2.8G with tele conversion lens MC7DGX and Nikkor28mm f/1.8 lenses were employed to image the turbulent flow for small and large measurement fields, respectively.

PIV measurements were taken for two measurement fields: A small measurement field through an 8 mm window with a 7 μm pixel size in the flow for high resolution; and a larger field through a 60 mm window with a 54 μm pixel size in the flow. The analysis window was set to 32 × 32 pixels with a 50% overlap for both measurement fields.

Figure 3 shows that the turbulence intensity is proportional to the fan speed. The turbulence was considered homogeneous with no regular bulk motion in the center of the combustion vessel [11]. The integral length scale of turbulence was determined by utilizing the data obtained from this PIV measurement.

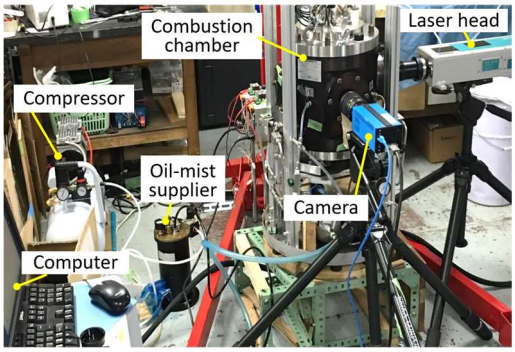

Fig. 2. Equipment of PIV measurement.

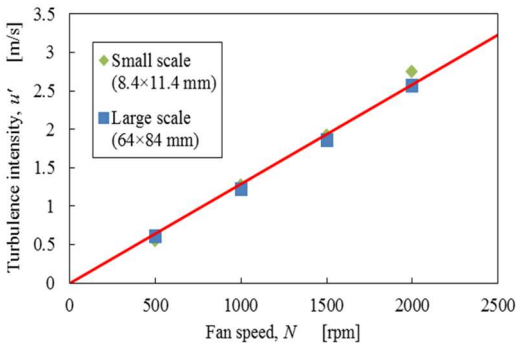

Fig. 3. Turbulence intensity, u' as a function of fan speed, N.

The data from the large measurement field was used to estimate the longitudinal integral length scale. Therefore, in this study, the distribution of turbulence intensity across the analysis area of 47 × 34 mm was adopted. The longitudinal velocity correlation coefficients, $R_{11}(x)$ were calculated using fluctuation components of velocity obtained from the PIV measurements. Hence, $R_{11}(x)$ was approximated by an exponential function as shown in (1),

$$R_{11}(x) \approx exp(-px^q) \tag{1}$$

where x is the separation distance along the horizontal axis of the turbulence intensity analysis area as shown in Fig. 4. The constants $p = 7.80 \times 10^{-3}$ and $q = 1.54$ were determined from the method of least-squares fits. The solid curve in Fig. 4 shows the approximated value of $R_{11}(x)$ according to (1). The longitudinal integral length scale, L_f is defined as the integration of $R_{11}(x)$ with respect to x from zero to infinity. Therefore, the integration can be determined using the Gamma function, Γ, as expressed in (2).

$$L_f = \int_0^\infty R_{11}(x)dx$$
$$= p^{-1/q} \cdot \Gamma(1 + 1/q) \tag{2}$$

A longitudinal integral length scale, L_f of 20.9 mm was calculated regardless of the turbulence intensity. The calculated L_f in this study was similar to the value obtained from previous studies

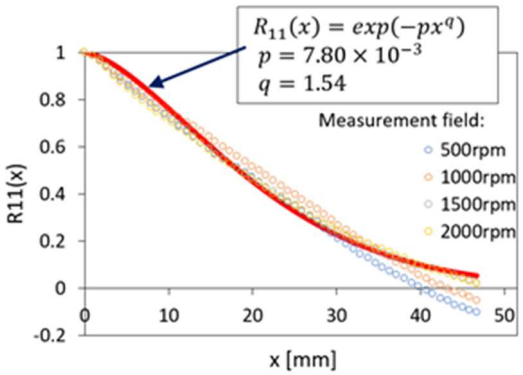

Fig. 4. Variation of longitudinal velocity correlation coefficient, $R_{11}(x)$, with distance, x.

[13,18]. The approach to determine the L_f value follows that of Smallbone et al. [11] and Hayakawa et al.[13].

3. Experimental results

3.1 Flame observation

Figure 5 shows sequential direct images of the spherical turbulent pulverized coal cloud flame propagation in a 40 vol% O_2 and 60 vol% N_2 gas mixture from the onset of ignition until 20 milliseconds (ms) for G = 2.0 kg/m^3. In this study, although partially irregular flame front shapes were observed, on the whole, the flame propagated almost spherically for all cases. Since the flame propagation velocity is relatively low in a coal particle cloud combustion, the flame front is highly deformed by turbulent eddies. Furthermore, the irregular shape of the flame front could be influenced by the heat loss to the electrodes in the horizontal direction, especially in the lower turbulence intensity cases. In addition, the various turbulent eddies acting on the reaction zone are expected to contribute to the irregular shape of the flame front, and there is a possibility that the turbulent eddies pull the flame front in the opposite direction of the flame propagation. Irregular shapes of flame front were also observed for gaseous hydrocarbon fuels in a turbulent field [18]. The flame diameter was determined by measuring the distance between the farthest flame fronts. As shown in Fig. 5, at

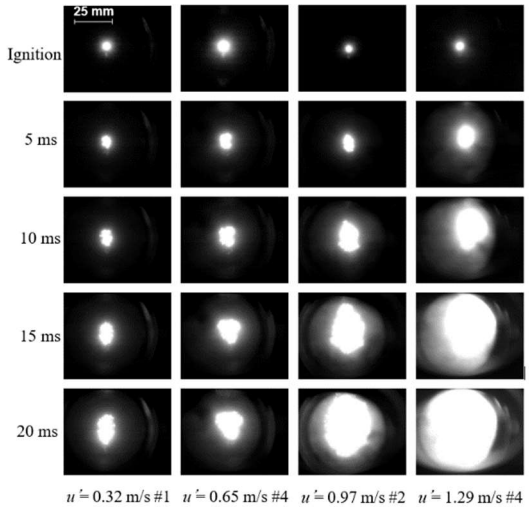

Fig. 5. Flame propagation in 40% O_2 and 60% N_2 mixture for G = 2.0 kg/m^3.

corresponding times (5, 10, 15 and 20 ms) from the ignition, the flame diameter increases as the turbulence intensity increases.

Figure 6 shows sequential spark images from the moment of electron discharge up to 5 ms for cases with and without a coal particle cloud. In Fig. 6(a), the small ball-shaped spark kernel is observed within the first few milliseconds and disappeared by 5 ms. On the other hand, as shown in Fig. 6(b), a larger spark kernel is observed at the onset, which is probably caused by the spark through the coal particles. Considering that the small spark kernel disappeared by 5 ms (Fig. 6(a)), whereas the larger kernel observed in Fig. 6(b) at 5 ms is a ”flame kernel” and is not a ”spark kernel”. Therefore, the first 5 ms can be treated as the ignition affected period.

Figure 7 illustrates the pressure history inside the chamber at u'= 0.32 m/s for the G = 1.3 kg/m^3 case. The pressure is within ± 5% of the atmospheric pressure after the dispersion of coal particles and remains almost constant up to 60 ms from the onset of ignition for all cases. Therefore, the pressure in

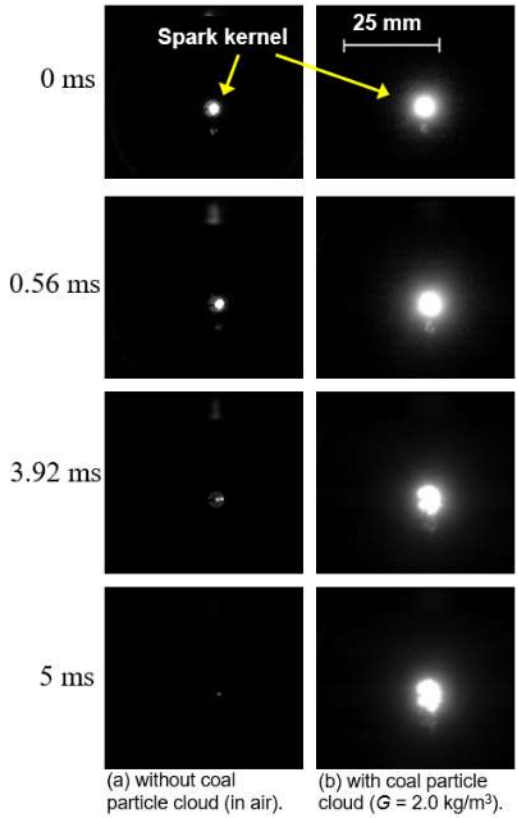

Fig. 6. Spark images (a) without coal particle cloud (in air) and (b) with coal particle cloud (u' = 0.32 m/s, G = 2.0 kg/m^3).

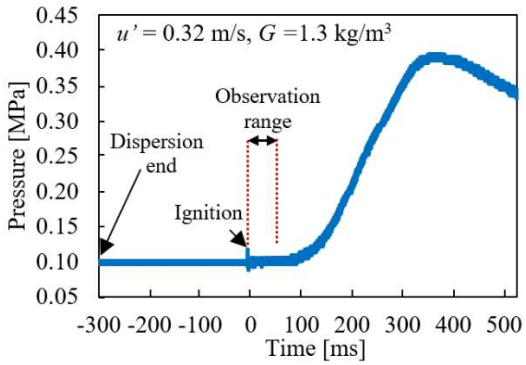

Fig. 7. Pressure history during flame propagation.

the chamber during the flame propagation within the observable range for flame radius measurements was assumed to be atmospheric pressure.

3.2 Flame propagation velocity

Figure 8 shows the flame radius time histories from 5 ms after the onset of spark ignition for various turbulence intensities for G=2.0 kg/m³. Although three experiments were performed for each condition, only one representative trace is shown for display purposes. It is assumed that the flame is not affected by the ignition spark after 5 ms. The ignition affected period was not considered in the measurement of flame radius. The flame radius was measured until the image of the flame front reached the edge of the window. Therefore, the maximum flame radius displayed in Fig. 8 does not indicate a final flame size, but indicates the limit of measurable flame radii due to the window size. As shown in Fig. 8, the flame radius increments rate increases as the turbulence intensity increases. Similar

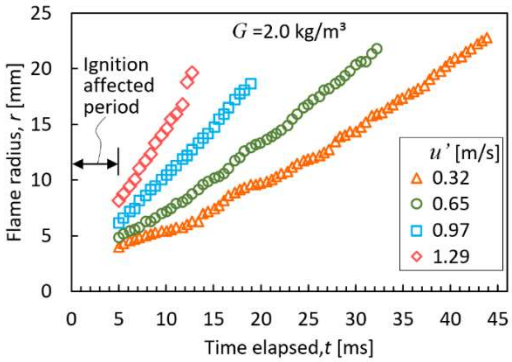

Fig. 8. Flame radius time histories for G = 2.0 kg/m³ in various turbulence intensity, u'.

trends were observed for all cases in this study.

Figure 9 shows the flame propagation velocity as a function of flame radius for various turbulence intensities. Similar to Fig. 8, only one flame propagation velocity trace was used in Fig. 9. The trend of flame propagation velocity was determined using a polynomial relationship of measured flame radius as a function of time. As shown in Fig. 9, for all coal concentrations, the flame propagation velocity increases with increasing flame radius. The observed acceleration is caused by a widening of the range of eddies that can increase the flame front area as the flame radius increases. Consequently, the number of eddies that wrinkle the flame front increases as the flame surface area increases. Thus, the heat and mass transfer rates increase causing the volatile matter release rate to increase as well. As a result, the flame propagation velocity increases.

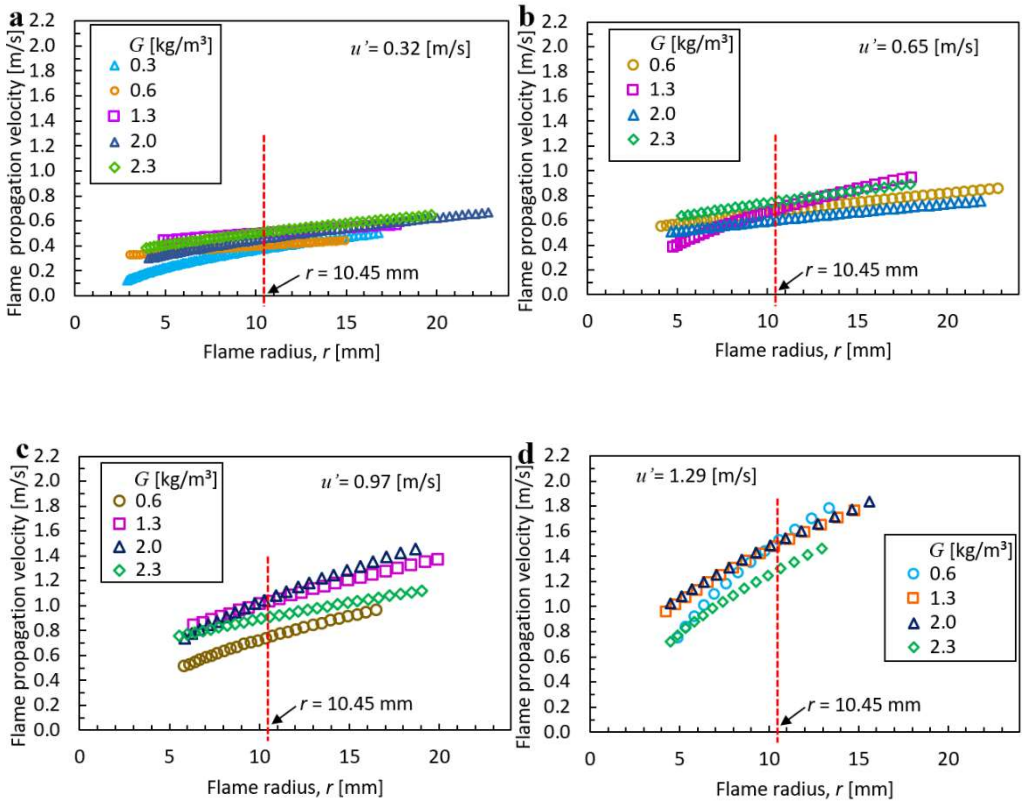

Fig. 9. Relationship between flame propagation velocity and flame radius for a) u'= 0.32 m/s, b) u'= 0.65 m/s , c) u'= 0.97 m/s and d) u'=1.29 m/s.

For all the cases in this study, the flame propagation velocity as a function of flame radius showed an increasing trend and did not reach any constant value within the observable range of flame radii. Fully developed velocity values were not obtained in this study. Therefore, following the approach of Mandilas et al. [19] and Kitagawa et al. [12], the flame propagation velocities at the flame diameter of 20.9 mm (radius of 10.45 mm), which is equivalent to the longitudinal integral length scale, L_f, calculated in the section 2.1, were used for the comparing the flame propagation velocities between different turbulence intensities.

In Fig. 9, the difference in the flame propagation velocity between the different coal concentration cases seems to have some trend. As mentioned earlier, however, only one representative trace for each case is shown for display purposes in Fig. 9. In Fig. 10, all of the measured flame propagation velocities at the flame radius of 10.45 mm are plotted, and no obvious trend was observed.

Figure 10 shows the effect of turbulence intensity on the flame propagation velocity at the flame radius of 10.45 mm for various coal concentrations. In general, the flame propagation velocity increases as the turbulence intensity increases regardless of coal concentration. As shown by Kitagawa et al.[12], for gaseous fuel, the flame propagation velocity increases as the turbulence intensity increases. They explained that increases in the flame propagation velocity were caused by increases in the flame front area by flame wrinkling due to turbulence. The same explanation can be adopted to the results of our study.

On the other hand, the coal concentration does not have an obvious effect on the flame propagation velocity. This tendency is different from that in the quiescent environment, in which the flame propagation velocity reaches a maximum value at a certain coal concentration as mentioned in Section 2. In a quiescent environment, the flame propagation velocity is mainly controlled by the heat conduction between gas and particles and the radiation between particles. In such a case, the distance between coal particles significantly affects flame propagation behavior. Therefore, the coal concentration, which determines the distance between coal particles, has a significant effect on the flame propagation velocity in a quiescent environment. In a turbulent environment, however, the flame propagation velocity is considered to be mainly dominated by turbulent heat transfer. Consequently, the flame propagation velocity increases as the turbulence intensity increases. The flame propagation velocity of a turbulent coal cloud is up to 5 times faster than that of the quiescent environment.

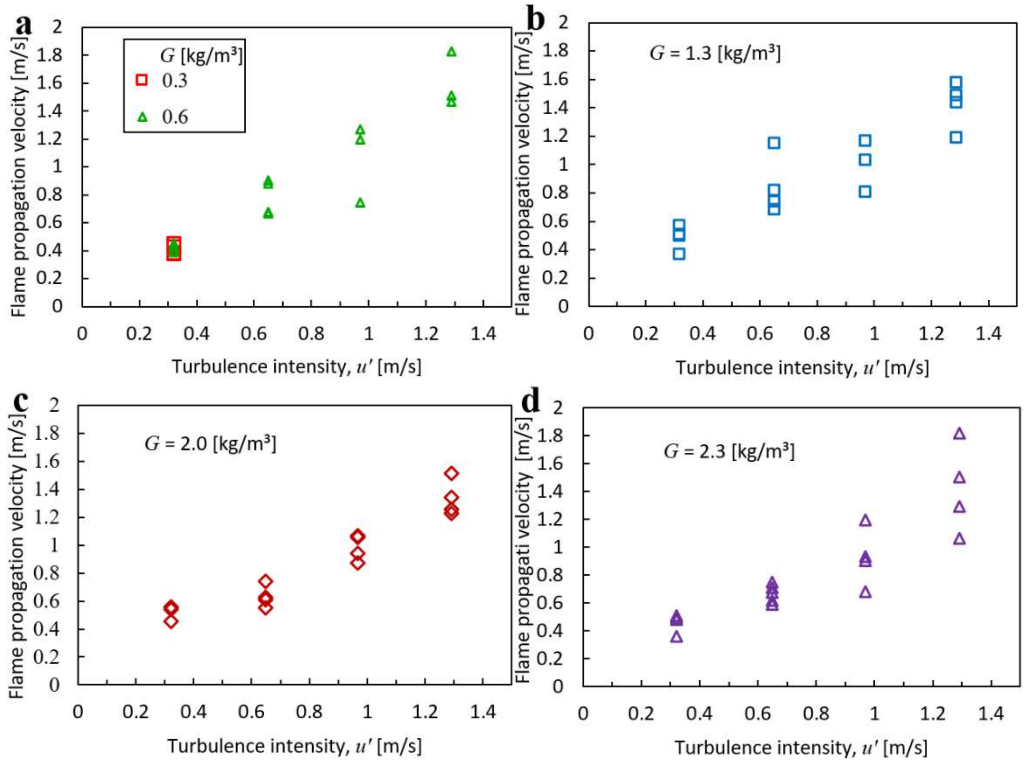

Fig. 10. Flame propagation velocity at various turbulence intensities, *u'* for a) *G* of 0.3 and 0.6 kg/m³, b) *G* =1.3 kg/m³, c) *G* = 2.0 kg/m³ and d) *G* = 2.3 kg/m³.

Accordingly, the effect of turbulence intensity on flame propagation velocity is dominant, and the effect of coal concentration is minimal. This is a unique feature of the flame propagation phenomenon in the turbulent field that was found in this research. In the quiescent coal particle cloud, flame propagation velocity has a maximum value at a specific coal concentration [1]. Significant effects of coal concentration on the flame propagation velocity were observed in pulverized coal particle combustion in laminar flow [2]. Moreover, in a gaseous fuel spherical flame propagation experiment, it was observed that the equivalence ratio strongly affects flame propagation velocity [12]. However, in a turbulent coal particle cloud, the flame propagation velocity is not much different for the various coal concentrations at a given turbulence intensity. According to Xu et al. [20], in the pulverized coal particle turbulent jet flame, eddies in the particle-loading turbulent jet strongly affect the ignition process, shortening the ignition delay time. However, there was no obvious effect of coal concentration on the ignition distance [20]. This tendency corresponds well with the results of our study.

As shown in Fig. 10, somewhat large scatter is observed at high turbulence intensity conditions. One reason for the large scatter is that the flame is highly deformed at high turbulence intensity conditions. A similar tendency has been observed in gaseous flame propagation [15,18]. A second reason for the scatter is that the effects of eddies on the flame propagation increase with increasing turbulence intensity. There are turbulent eddies with various sizes in the turbulent flow field and the wrinkling effects of each eddy size is different. Therefore, the nonuniformity of the wrinkling effects of eddies increases with increasing turbulence intensity.

4. Conclusions

Experimental results of the spherical flame propagation behavior of turbulent pulverized coal particle clouds has been reported for the first time. The effect of turbulence intensity and coal particle concentration on the flame propagation behavior of pulverized coal particle cloud at atmospheric pressure were clarified. The primary findings were as follows:

1. The flame propagation velocity of a pulverized coal particle cloud is increased with increasing flame radius in a turbulent field. This is caused by a widening of the range of eddies that serve to increase the flame front area as the flame radius increases, as expected in gaseous fuel combustion.
2. The flame propagation velocity of a pulverized coal particle cloud is increased as the turbulence intensity increases. This tendency can be explained by the increase in turbulent heat transfer rate at the flame front as the turbulence intensity increases.
3. Compared to the turbulence intensity, the coal concentration has a weak effect on the flame propagation velocity, which is a feature that is unique to pulverized coal flames in a turbulent field. This finding is one of the major contributions of this study in that it is obviously different from the results observed in previous pulverized coal combustion studies, as well as that of gaseous fuel combustion research.

5. Acknowledgment

Part of this work was supported by JST research promotion program Sakigake (PRESTO) Grant Number JPMJPR1542. The authors are indebted to Dr. Suda of IHI Co., Prof. Kitagawa of Kyushu Univ., Prof. Hayakawa of Tohoku Univ. for their helpful advice and discussion. The authors also indebted to the Central Research Institute of Electric Power Industry for providing coal particle samples.

References

[1] T. Suda, K. Masuko, J. Sato, A. Yamamoto, K. Okazaki, Fuel 86 (2007) 2008–2015.

[2] M. Taniguchi, H. Kobayashi, K. Kiyama, Y. Shimogori, Fuel 88 (2009) 1478–1484.

[3] O. Fujita, K. Ito, T. Tagashira, J. Sato, Heat Transfer in Microgravity 269 (1993).

[4] T. Kiga, S. Takano, N. Kimura, K. Omata, M. Okawa, T. Mori, M. Kato, Energy Convers. Manag. 38 (1997) S129–S134.

[5] S.M. Hwang, R. Kurose, F. Akamatsu, H. Tsuji, H. Makino, M. Katsuki, Energy and Fuels 19 (2005) 382–392.

[6] R. Kurose, M. Ikeda, H. Makino, M. Kimoto, T. Miyazaki, Fuel 83 (2004) 1777–1785.

[7] J. Hayashi, N. Hashimoto, N. Nakatsuka, H. Tsuji, H. Watanabe, H. Makino, F. Akamatsu, Proc. Combust. Inst. 34 (2013) 2435–2443.

[8] N. Hashimoto, J. Hayashi, N. Nakatsuka, K. Tainaka, S. Umemoto, H. TSUJI, F. Akamatsu, H. Watanabe, H. Makino, J. Therm. Sci. Technol. 11 (2016) JTST0049-JTST0049.

[9] M. Taniguchi, H. Kobayashi, S. Auhata, Symp. Combust. 26 (1996) 3189–3195.

[10] J. Krüger, N.E.L. Haugen, D. Mitra, T. Løvås, Proc. Combust. Inst. 36 (2017) 2333–2340.

[11] A. Smallbone, K. Tsuneyoshi, T. Kitagawa, J. Therm. Sci. Technol. 1 (2006).

[12] T. Kitagawa, T. Nakahara, K. Maruyama, K. Kado, A. Hayakawa, S. Kobayashi, Int. J. Hydrogen Energy 33 (2008) 5842–5849.

[13] A. Hayakawa, Y. Miki, Y. Nagano, T. Kitagawa, J. Therm. Sci. Technol. 7 (2012) 507–521.

[14] S.D. Tse, D.L. Zhu, C.K. Law, Proc. Combust. Inst. 28 (2000) 1793–1800.

[15] J. Goulier, N. Chaumeix, F. Halter, N. Meynet, A. Bentaïb, Nucl. Eng. Des. 312 (2017) 214–

227.

[16] S.S. Shy, Y.W. Shiu, L.J. Jiang, C.C. Liu, S. Minaev, Proc. Combust. Inst. 36 (2017) 1785–1791.

[17] A. Hayakawa, T. Goto, R. Mimoto, Y. Arakawa, T. Kudo, H. Kobayashi, Fuel 159 (2015) 98–106.

[18] D. Bradley, M.Z. Haq, R.A. Hicks, T. Kitagawa, M. Lawes, C.G.W. Sheppard, R. Woolley, Combust. Flame 133 (2003) 415–430.

[19] C. Mandilas, M.P. Ormsby, C.G.W. Sheppard, R. Woolley, Proc. Combust. Inst. 31 I (2007) 1443–1450.

[20] K. Xu, Y. Wu, Z. Wang, Y. Yang, H. Zhang, Fuel 167 (2016) 218–225.